Biomechanics of Abdominal Aortic Aneurysm in the Presence of Endoluminal Thrombus: Experimental Characterisation and Structural Static Computational Analysis

E. Di Martino*[1,3], S. Mantero[1,3], F. Inzoli[2,3], G. Melissano[4], D. Astore[4], R. Chiesa[4] and R. Fumero[1,3]

[1]*Dipartimento di Bioingegneria, Politecnico di Milano,* [2]*Dipartimento di Energetica, Politecnico di Milano,* [3]*CeBITeC, IRCCS H.S. Raffaele, Milano,* [4]*Istituto Malattie Apparato Cardiovascolare e Respiratorio, Università di Milano, Divisione Chirurgia Vascolare IRCCS H.S. Raffaele, Milano, Italy*

Objectives: To evaluate the role played by biomechanical and geometrical parameters of endoluminal thrombus and of aortic wall on abdominal aortic aneurysm (AAA) behaviour.
Materials and methods: Tensile tests on 21 AAA thrombus specimens from six patients undergoing AAA repair and numerical evaluation of aneurysmal aortic wall stress and strain distribution. Parameters of the analysis were lumen eccentricity, thrombus Young's Modulus and the aortic wall constitutive equation.
Results: There was a linear stress/strain for all the thrombus specimens. The numerical analyses show the mechanical behaviour of AAA as a function of lumen eccentricity and biomechanical parameters.
Conclusions: Well organised thrombus reduces the effect of the pressure load on the aneurysmal aortic wall.

Key Words: Abdominal aortic aneurysm (AAA); Endoluminal thrombus; Thrombus mechanical properties; Aneurysm mathematical model.

Introduction

The predominant aetiology of abdominal aortic aneurysms (AAA) is thought to be an ongoing weakening of the aortic wall. Two principal constitutive elements contribute to aortic wall structure, collagen and elastin, which play different roles in maintaining wall integrity and elasticity. This is due to their different mechanical properties: elastin sustains the pressure load under physiological conditions due to its high stretching and elastic capabilities, while collagen is involved when additional pressure load is applied to the aortic wall, and it reacts with a stiffer behaviour in order to maintain the aortic diameter within physiological acceptable values. In AAA, a reduction of the thickness of the aortic wall due to elastin and collagen degeneration is observed.[1-6] Moreover, the alteration of the haemodynamic milieu causes recirculation and stagnation, which may contribute to the formation and progress of an endoluminal thrombus.

The stability of an AAA is linked to the aortic pressure levels, to the stress patterns in the aneurysm aortic wall and to the shape (fusiform or saccular) of the aneurysm itself. Some of these parameters can be evaluated using diagnostic methodologies such as computer tomography (CT) and magnetic resonance imaging (MRI). These techniques allow the evaluation of some parameters that describe the geometry of AAA, such as longitudinal extension of the aneurysm, aortic diameter, luminal diameter, thickness of the aortic wall and the calcifications of the aortic wall; it is also possible to evaluate the presence of a thrombus and lumen eccentricity. Some of these parameters are used as decisional indices.[7,8]

The prognosis of patients with AAA is often critical because of dissection and rupture of the aortic wall, and although the risks of elective AAA repair are decreasing, the choice of the appropriate treatment requires a careful evaluation of the surgical risks versus the risks of rupture of the AAA. Although it has been clearly established that elective resection of AAA gives the patient the best chance of survival, caution must be exercised before advising aneurysm repair for the poor-risk patient.[9-11] The evaluation of rupture risk is based upon geometric information (location and maximum diameter) and the characterisation of the

---

* Please address all correspondence to: E. Di Martino, Dipartimento di Bioingegneria, Politecnico di Milano, Piazza Leonardo da Vinci, 32 20133 Milano, Italy.

Table 1. Patient age, lumen eccentricity and maximum aortic diameter obtained from MRI examination, and number of samples tested for each patient.

Patient	Age	Lumen position	Maximum aneurysm diameter (cm)	Number of specimens
A	70	Eccentric	5	1
B	77	Concentric	5.5	3
C	67	Eccentric	7.5	5
D	67	Concentric	7	3
E	88	Eccentric	8	5
F	62	Concentric	6	4
Mean	71.8	—	6.5	
S.D.	8.5	—	1.18	

endoluminal thrombus, if present. Nonetheless, aneurysms with diameter greater than 5–7 cm can be stable while smaller ones can experience fast growth and rupture.[12]

A detailed knowledge of wall stress distribution could allow the prediction of the aneurysm evolution and its eventual rupture, as suggested by the results of a previous work.[13] In this study characterisation of the wall stresses of an axisymmetric aneurysm model was performed using the finite element method (FEM). The presence of the thrombus and the properties of the wall (e.g. presence of atherosclerotic plaque) modified the maximum stress values and locations, the thrombus reducing the overall stress and the plaques causing stress concentration. As for aneurysm geometry, the maximum stresses have been found at the aneurysm neck for larger diameter aneurysms and at the site of maximum dilation for smaller diameter.

Mechanical characterisation of the aortic wall, both physiological and pathological has been described in literature,[14–16] however mechanical characterisation of the thrombus has not. In this work, monoaxial tensile properties of aortic thrombus are documented in order to provide data about thrombus constitutive equation that can be used to implement mathematical models of the AAA mechanical behaviour. Using the experimental results of the mechanical tests, a mathematical analysis has been performed on bidimensional AAA in order to evaluate the role of thrombus and aortic wall mechanical properties and of the eccentricity of the patent lumen, on the stress and strain distribution of the aneurysmatic aortic wall. This model allows us to obtain information about the aortic wall stress and strain distribution on the transversal plane of the aneurysm, which can be useful to complete the data on the longitudinal distribution of aortic wall stresses obtained with the axisymmetric models of the aneurysm.[13]
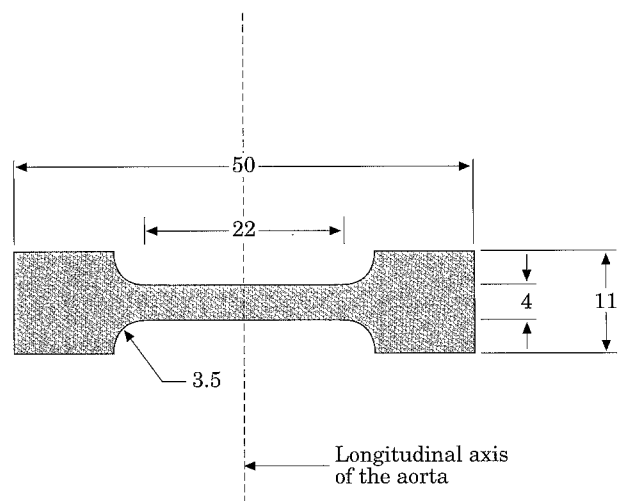

Fig. 1. Shape of the specimens used to perform mechanical monoaxial tests on thrombus material. The thrombus specimens were cut in circumferential direction.

Materials and Methods

Experimental test

Mechanical monoaxial tensile tests were carried out on 21 specimens prepared from aortic thrombus removed from six male patients during elective surgical resection of AAA. In order to perform mechanical characterisation of thrombus material, only well-organised thrombi were selected for testing. Table 1 shows the patient age, the results of MRI examination and the number of specimens tested for each patient.

During surgery the thrombus was removed and stored in 0.9% saline solution at 4 °C before testing. All mechanical tests were performed within 24 h of removal. For all patients circumferentially cut specimens were obtained from the thrombus. A custom designed die whose shape is shown in Fig. 1 was used
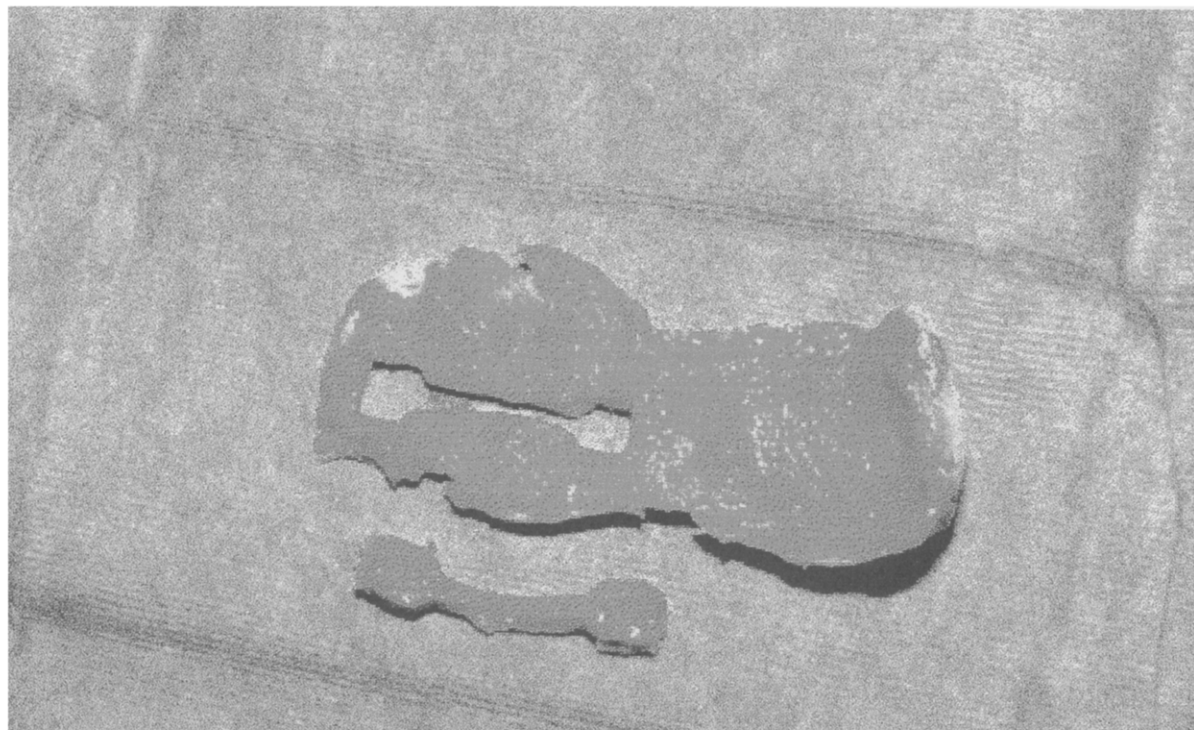
Fig. 2. Photograph of a specimen cut from the luminal portion of the thrombus.

to cut tensile specimens from thrombus strips. After cutting, the specimens were mechanically tested using an Instron 4505. The tests were performed with a cross-bar speed of 20 mm/min at 23 ± 1 °C.

The thickness of each specimen was evaluated using a micrometer gauge; the average specimen's cross-section was 14.5 ± 3 mm^2. The samples were gripped by ribbed clamps to prevent them from slipping during the test. Figure 2 shows a photograph of a luminal portion of a thrombus with a specimen circumferentially cut. Engineering tensile strain (ε) was calculated as $\varepsilon = \Delta L / L_o$ where L_o is the original zero-loaded grip distance and ΔL is the grip displacement from the zero-load position. Engineering tensile stress (σ) was calculated as $\sigma = F/A_o$ where F is the applied force, and A_o is the original sample section.

Numerical simulation model

A mathematical model of the transverse section of the aneurysmatic wall with the endoluminal thrombus was studied. The 2D simplified model allowed us to evaluate how lumen eccentricity and mechanical properties of the thrombus and of the aortic wall affect the investigated variables (the aortic wall stress and strain). The reference 2D model can be described by four variables: external diameter of the aorta, aortic
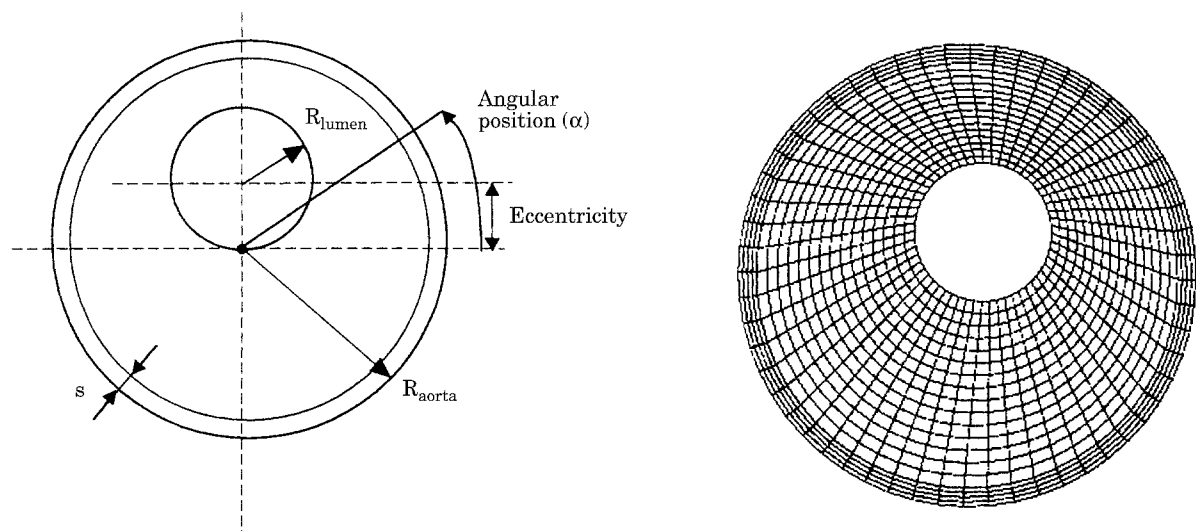
wall thickness, diameter of the lumen and eccentricity of the lumen. The study was performed assuming the following constant values as a reference unloaded configuration: aneurysm diameter $2R_{aorta} = 5$ cm, lumen diameter $2R_{lumen} = 1.5$ cm and aortic wall thickness $s = 2$ mm. The eccentricity (0–15 mm) was used as a parameter for the analysis to investigate its role in wall stresses development.

An additional model was developed modifying the eccentricity axis with respect to the spine by 90°. This occurrence is not frequent in clinical practice, but it is interesting to compare its influence on the stress distribution results. Table 2 resumes the aneurysm models analysed. In this table the eccentricity of the lumen is identified as the distance between the centre of the aortic vessel and the centre of the patent lumen.

Figure 3 shows a schematic representation of the model and the finite elements used for the structural analysis. The model is made of quadrilateral isoparametric elements with four nodes for both the aortic wall and the thrombus: a total amount of 223 elements were used for the wall in the different models and about 920 elements were used for the thrombus. The boundary conditions consist of a two degrees of freedom (DOF) constraint (hinge) simulating the presence of the dorsal spine and a one DOF constraint opposite to the previous one, which allows only radial movements. The load applied to all the models analysed

Table 2. Models analysed, eccentricity values of the patent lumen and eccentricity axis location.

Model	Eccentricity (mm)	Eccentricity axis location (angle between geometrical symmetry axis and eccentricity axis)
Model__0	0	0
Model__5	5	0
Model__10	10	0
Model__15	15	0
Model__90	10	90

Fig. 3. Sketch of the bidimensional model of the abdominal aortic aneurysm (left) and mesh of the solid domain (right).

was a normal incremental pressure of 120 mmHg on the internal side of the lumen.

Data about the mechanical properties of the aorta come from previous experimental studies.[12,16-18] Human arterial tissue exhibits non-linear behaviour both in physiological and pathological conditions. In order to evaluate the stress fields on an aneurysmal abdominal aortic wall we used a non-linear stress/strain characteristic referred to pathological aortic specimens.[18]

Another set of simulations was performed using a linearisation of the aortic wall stress/strain characteristic over a physiological range. The adopted values for these set of simulations were E = 1 MPa for the Young's Modulus and $\nu = 0.5$ for Poisson's Modulus.[12,16,17] This appears to be consistent when dealing with a healthy wall because the stress/strain curve exhibits a large portion of linear elastic behaviour that can therefore be linearised about the working point. The same approach is not feasible when the studied wall is aneurysmal, because the stress/strain curve exhibits a more strict non-linear behaviour due

to stiffening at low strain values. A non-linear description of the aneurysmal aortic wall behaviour was therefore used. A comparison can be performed between the results of the two sets of simulation assuming that the non-linear simulation accounts for the aneurysmatic wall characteristics as measured by Roach et al.[18] and the linear simulation refers to a non-degenerate aortic wall.

For the thrombus the mechanical properties obtained from the experiments previously described were used. In particular, the mean values of the Young Modulus (E) were used with a Poisson's Modulus of 0.5. A sensitivity set of analyses was performed to investigate to what extent the wall stresses are modified by different values of thrombus Young's Modulus. In this preliminary work, steady state analyses have been performed to assess the effectiveness of the computational approach. Further studies are being carried out in order to assess the effect of blood pulsatility in the AAA model.

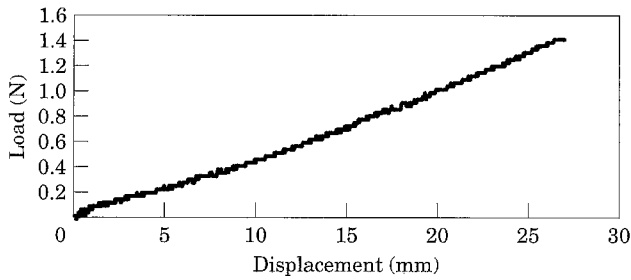The study was performed using CAD techniques, involving mesh creation, solution of the static analysis

Fig. 4. Example of a load/displacement curve obtained from the experimental tensile test performed on one thrombus specimen. The behaviour is linear following Hooke's law, $\sigma = \varepsilon E$.

with FEM and post-processing of results. The first step of the computational approach was the 2D solid modelling of the AAA for which we used the commercial code Pro/Engineer (Parametric Technology Corporation, Waltham, MA, U.S.A.). The solid model was transferred from the CAD code to a mesh generator program to create the discrete model. Both the thrombus and the aortic wall were meshed using 4-node elements. P3/Patran (MSC, Costa Mesa, CA, U.S.A.) was the commercial code used to generate the mesh. The meshes were transferred to ABAQUS (Hibbit, Karlsson & Sorensen Inc., Pawtucket, RI, U.S.A.) code which is a commercial code for FEM structural analysis. The mathematical formulation of the problem required the use of non-linear steady Lagrange equilibrium equations.[19] ABAQUS uses the Newton method as a numerical technique to solve the non-linear equilibrium equations. By expanding the equations of the non-linear system in a Taylor series about the approximate solution, the method allows a linear system of equation to be handled instead of the non-linear one. For unstable problems a modified Newton method is available in ABAQUS. The latter was used to reach non-linear static equilibrium. The load increment size is determined by this algorithm and it is convergence rate dependent in order to have the best increment each step.[20]

Results

For each specimen a load-displacement curve was recorded. Figure 4 shows an example of a load-displacement diagram obtained from patient F. The relationship between load and displacement was found to be linear (r>0.99) for all the patients. Therefore the equation governing the thrombus material behaviour is the Hooke relation, in which the proportional constant between stress (σ) and strain (ε) is the Young's Modulus (E), that is $\sigma = E\varepsilon$.

Table 3. Results of the mechanical tests performed on thrombus specimens.

Sample	Ultimate stress (MPa)	Ultimate deformation	Young's Modulus (MPa)
A1	0.047	0.564	0.083
B1	0.021	0.481	0.042
B2	0.019	0.335	0.057
B3	0.041	0.726	0.055
C1	0.092	0.545	0.168
C2	0.161	0.875	0.184
C3	0.033	0.355	0.094
C4	0.078	0.678	0.115
C5	0.081	0.387	0.208
D1	0.020	0.433	0.046
D2	0.071	0.782	0.091
D3	0.116	0.869	0.134
E1	0.089	0.9	0.099
E2	0.118	0.911	0.129
E3	0.109	0.727	0.151
E4	0.061	0.648	0.093
E5	0.067	0.623	0.108
F1	0.171	0.817	0.209
F2	0.087	0.388	0.22
F3	0.171	0.628	0.271
F4	0.129	0.691	0.187
Mean	0.085	0.636	0.131
S.D.	0.047	0.187	0.064

Table 3 shows the complete results of the mechanical tests performed. For all samples ultimate stress, strain and Young's Modulus values are reported. Ultimate stress and strain are the measured values for stress and strain at the time of the specimen rupture. Figure 5 shows the Young's Modulus values for all the samples analysed. The range of variability for the specimens' Young's Moduli was 0.05–0.2 MPa.

To present the results of the computational analyses we used stress fields plotted on the geometric model of AAAs and polar diagrams that can resume in a unique diagram the results of different simulations. Polar diagrams represent the maximum deformation or the maximum stress on the aortic wall with respect to an angular position (α) relative to the symmetry axis through the spine. The results obtained from the FEM simulations show that the maximum aortic wall
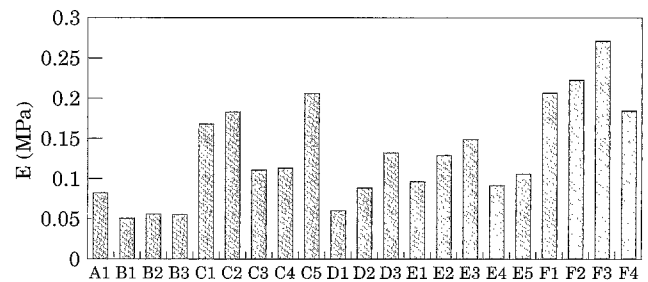

Fig. 5. Histogram showing the Young's Modulus value for all thrombus samples tested.

stress changes as a function of the eccentricity of the patent lumen.

The aim of the analyses was to provide information about the risk of rupture of the aneurysmal aortic wall when geometric and biomechanic characteristics are changed. The maximum tensile strain theory has been demonstrated to give reliable information about the failure of the aortic tissue.[21] Thus the polar diagrams report the maximum circumferential strain on the aortic wall. As for the stress variables, the principal stresses were chosen to correlate with the strain measures.

Figures 6 and 7 show the contours of the principal stress fields in radial and circumferential direction respectively, on the aneurysmal aortic wall and on the thrombus at different values of lumen eccentricity. The results of the simulation performed on the model with a concentric lumen showed a uniform distribution of principal stresses on the thrombus and on the aortic wall. The results of the simulations on the eccentric models of the aneurysm showed how, as the thickness of the thrombus reduced, the wall exhibited an increasing stress both in the radial and in the circumferential directions. The maximum stress concentration was localised on the aortic wall corresponding to the area of minimum thrombus thickness.

Figure 8 shows polar diagrams representing the maximum deformation of the aortic wall for all the models. Each point of the polar diagram represents the maximum deformation on the aortic wall at a defined angular location and for a defined model. The left side of the diagram refers to the results of the simulations performed for an aneurysmal aortic wall and the right side of the diagram refers to the results of the simulation performed for a normal aortic wall. Figure 9 shows the stress polar diagram for two models with equal eccentricity and different direction of eccentricity. Figure 10 shows the aortic wall circumferential stresses as a function of the thrombus thickness for an aneurysmal aortic wall and for a normal one. The relation between thickness and stress was approximately exponential, indicating that a reduction of thrombus thickness, with a constant lumen diameter, can increase the risk of wall rupture.

Discussion

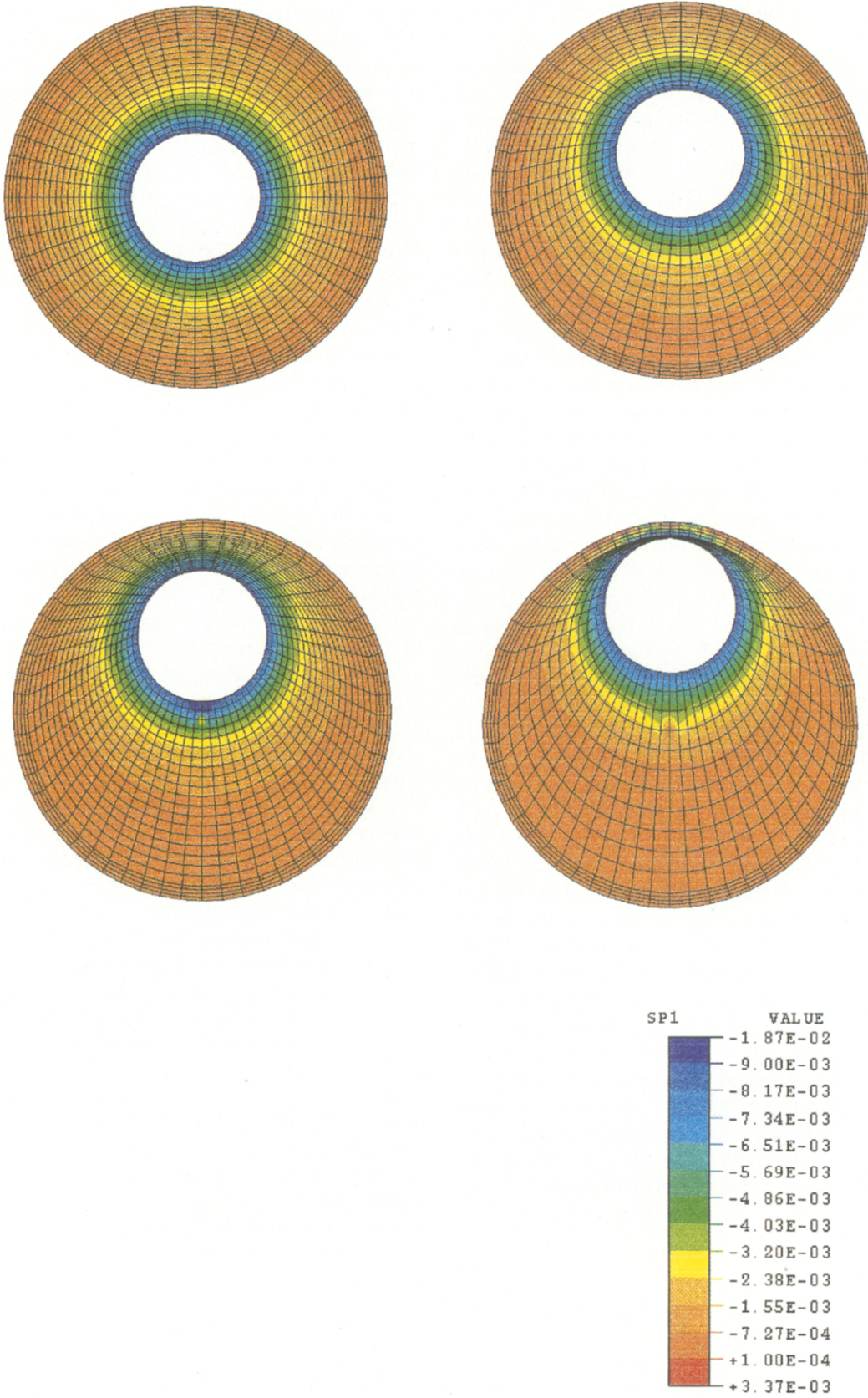Clinical observations have suggested that the endoluminal thrombus may play a fluid dynamic role in maintaining fluid physiological blood velocity within the aneurysmal vessel and a mechanical role in preserving the aneurysm wall from rupture.[11] At the time of surgery the thrombus is observed as an organised or non-organised structure, which affects the mechanical properties. Diagnostic examination (MRI) can sometimes predict its character.[22] The mechanical experiments performed on thrombus specimens allowed us to obtain elastic properties of this tissue in terms of Young's Modulus values; these values have been used to implement a realistic mathematical model of AAA.
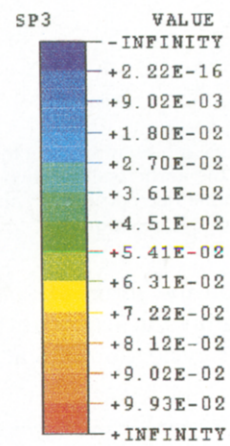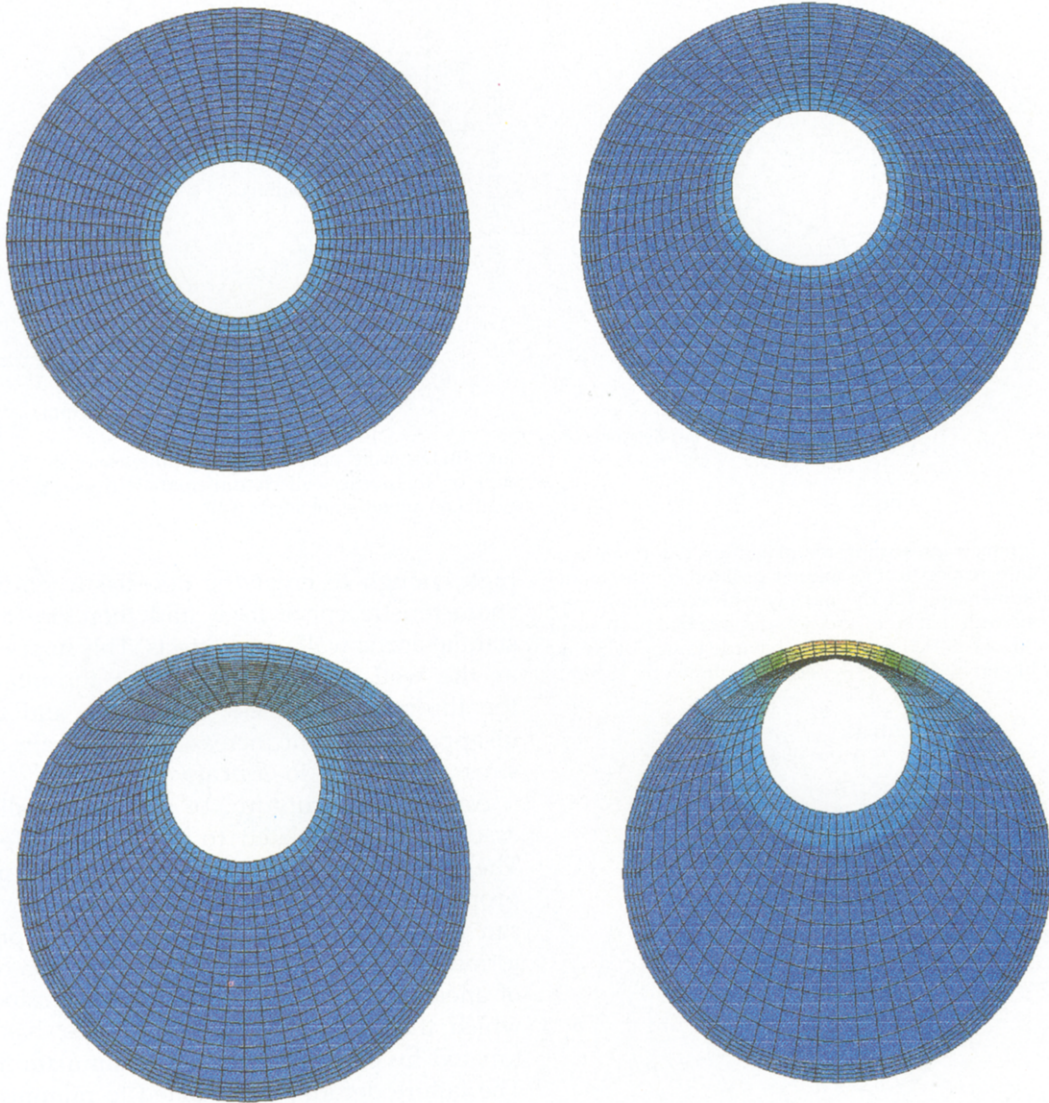
There are two limitations in this experimental study: the small number of samples obtained from each patient and the lack of reliable measurements of specimen thickness. The instruments allow only a poor quantification of specimen thickness because of the non-uniform thickness and non-homogeneous composition of the tissue. As a consequence the measured values for the stresses are affected by the measurements of the cross-section. Nonetheless, consistent characterisation of the thrombus has been attained, as will be discussed later.

Electron microscopy reveals the thrombus structure to be multi-layered. This structure suggests a sequential development of the thrombus, following lumen expansion, in an attempt to normalise physiological fluid dynamic variables, such as pressure and velocity. In turn, the degenerate and dilated aneurysmal aortic wall undergoes wall thickness reduction and tissue degeneration that can lead to aneurysm rupture. The thrombus formation may be therefore involved in two phenomena: on one hand it preserves wall integrity, while on the other hand it maintains the original lumen diameter and hence the previous fluid dynamic conditions. The numerical experiments performed corroborate this hypothesis about the active role played by the thrombus formation in preserving aortic wall integrity by means of a reduction of the stresses acting on the aortic wall itself (Figs 6 and 7).

The results obtained simulating the absence of organised thrombus show considerably higher values for circumferential aortic wall maximum stress when the aortic wall is aneurysmal (Fig. 10). The finding that the stresses on the aneurysmal wall are, in absolute terms, less than those calculated for the normal aorta (Fig. 8) may be puzzling, but it must be pointed out that the aneurysmal wall is much more rigid due to the elastin degeneration. The stress/strain characteristic for an aneurysmal wall is therefore shifted

---

Fig. 6. (*overleaf*) Contours of the principal stress fields in radial direction (MPa) on the aortic wall and on the thrombus for the aneurysm model with concentric lumen and for the aneurysm models with eccentric lumen, in which the aortic wall stress/strain characteristic has been assumed non-linear.
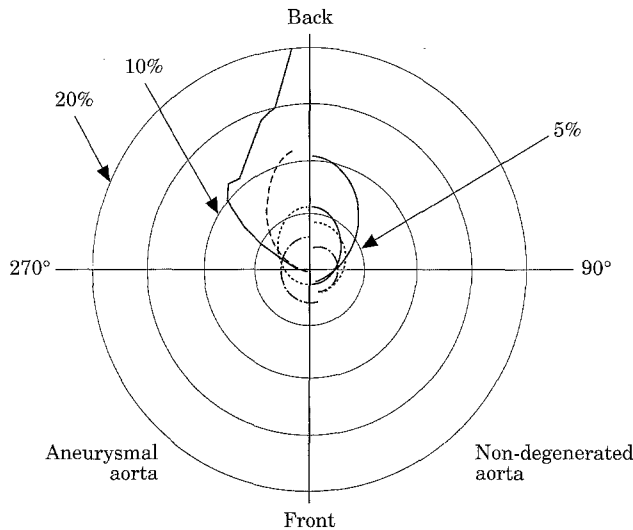
SP1	VALUE
	-1.87E-02
	-9.00E-03
	-8.17E-03
	-7.34E-03
	-6.51E-03
	-5.69E-03
	-4.86E-03
	-4.03E-03
	-3.20E-03
	-2.38E-03
	-1.55E-03
	-7.27E-04
	+1.00E-04
	+3.37E-03

Fig. 10. Diagram representing the influence of the thrombus thickness on the aortic wall circumferential stress. (■) Normal aortic wall; (▲) aneurysmal aortic wall.

Fig. 8. Polar diagrams representing the maximum deformation of the aortic wall with respect to the angular position for the model with concentric lumen and for the models with eccentric lumen. Aneurysmal aortic wall (left side) and non-degenerated aortic wall (right side). (—·—) Concentric lumen; (....) eccentric lumen by 5 mm; (———) eccentric lumen by 10 mm; (—) eccentric lumen by 15 mm.
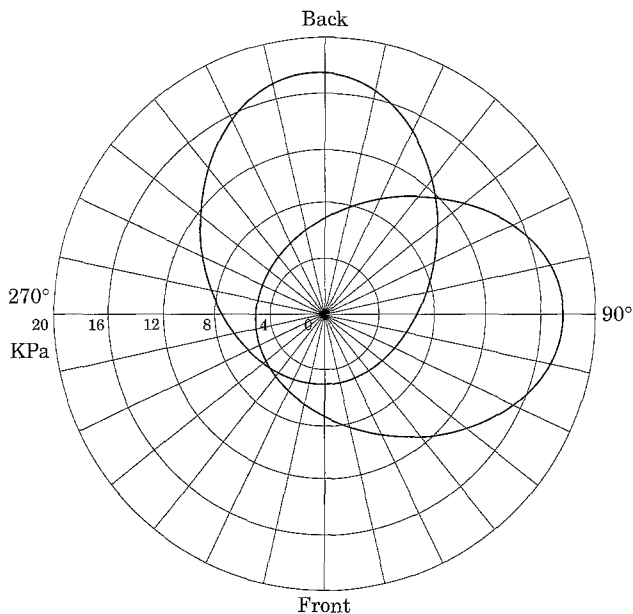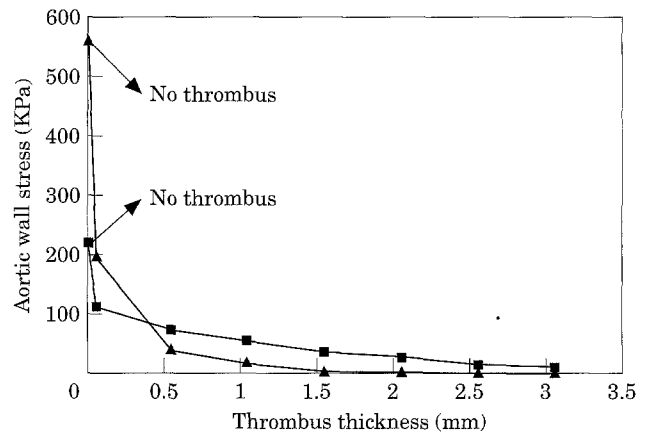

Fig. 9. Polar diagrams representing the maximum deformation values calculated on the aortic wall for two models characterised by different axes of lumen eccentricity, 0° and 90° with respect to the symmetry axis through the spine.

towards the left on the strain axis. As a consequence the stress and strain values around the working point, during the cardiac cycle, do not reach values of strain

high enough to enter the non-elastic portion of the characteristic curve itself and therefore avoid substantial aortic wall creep effects. This happens as long as the wall is protected by the thrombus, but as the thrombus thickness diminishes and eventually disappears, a slight increase in the strain causes the stress to increase to critical values.

An index of "rupture" of the aortic wall has been assumed to be related to the vessel deformation.[21] The simulations that we performed have parametric properties. The mean peak pulse pressure value used can be therefore modified in order to provide information about the effect of hypertension on the risk of aneurysm rupture. A critical strain value, beyond which the aneurysmal wall ruptures, has been estimated by performing a failure simulation of AAA. The failure deformation, related to minimum thrombus thickness, is 57% and the related pressure is 250 mmHg. The deformations obtained at a mean peak pressure of 120 mmHg (Fig. 8) can be therefore related to the failure deformation of the aortic wall.

The results obtained by moving the axis of eccentricity of the lumen from the axis through the spine constraint and the vessel centre to a perpendicular axis show that the stress distribution on the aortic wall is equally rotated by 90°, as shown in Fig. 9. This means that, with the constraints given, the thrombus thickness represents the major factor determining the aortic wall stresses. The model appears not to be sensitive to the mechanical constraint imposed by the presence of the vertebral spine. However, this situation may introduce friction between the spine and the

Fig. 7. (*overleaf*) Contours of the principal stress fields in circumferential direction (MPa) on the aortic wall and on the thrombus for the aneurysm model with concentric lumen and for the aneurysm models with eccentric lumen, in which the aortic wall stress/strain characteristic has been assumed non-linear.
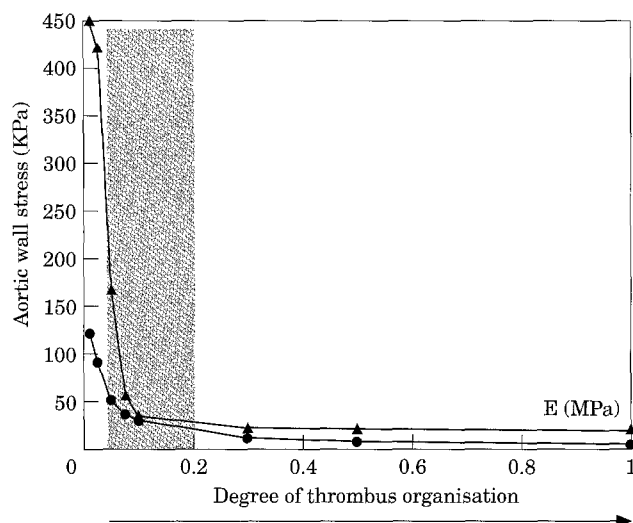
Fig. 11. Diagram representing the influence of the mechanical properties of the thrombus (Young's Modulus) on the maximum aortic wall circumferential stress. The model used for the sensitivity analysis has a concentric lumen. In light grey is the range of thrombus Young's Modulus variability found in the experimental tests. (▲) Aneurysmal aortic wall; (●) normal aortic wall.

aneurysmal wall (instead of a simple hinge constraint), which may contribute to wall rupture.

The Young's Modulus values obtained from the tensile tests on the thrombus specimens ranged between 0.05 and 0.27 MPa with a standard deviation that, within the specimens of the same patient, ranged between 0.002 and 0.04 MPa. A sensitivity analysis has been performed modifying the Young's Modulus value on a concentric aneurysmatic model and the maximum absolute values of the stresses on the aortic wall are shown in Fig. 11. In the same figure the experimental Young's Modulus range of variability is shaded light grey. This diagram shows clearly how the organisation of the thrombus, which is correlated to its mechanical characteristics, lowers the stress on the aortic wall. This effect is greater if the aortic wall is degenerate.

In conclusion, these results show how the presence of the thrombus, the mechanical properties of the thrombus and the eccentricity of the patent lumen influence the aortic wall stress distribution and values. The thicker the thrombus layer, the less the surrounding wall is stressed. The results of this work could be useful in understanding how lumen eccentricity, thrombus properties and aortic wall composition contribute to the natural evolution of AAA and in particular to the events associated with rupture.

References

1 BAXTER BT, McGEE GS, SHIVELY VP, DRUMMOND IAS, DIXIT SN, YAMAUCHI M, PEARCE WH. Elastin content, cross-link, and

mRNA in normal and aneurysmal human aorta. *J Vasc Surg* 1992; **16**: 192–200.

2 HAYASHI K. Experimental approaches on measuring the mechanical properties and constitutives laws of arterial walls. *J Biomech Eng* 1993; **115**: 481–487.

3 ANIDJAR S, DOBRIN PB, CHEJFEC G, MICHEL JB. Experimental study of determinants of aneurysmal expansion of the abdominal aorta. *Ann Vasc Surg* 1994; **8**: 127–136.

4 MESH CL, BAXTER TB, PEARCE WH, CHISHOLM RL, McGEE GS, YAO JST. Collagen and elastin gene expression in aortic aneurysms. *Surgery* 1992; **112**: 256–262.

5 BUSSUTIL RW, ABOU-ZAMZAM AM, MACHLEDER HI. Collagenase activity of the human aorta. *Arch Surg* 1980; **115**: 1373–1378.

6 MACSWEENEY STR, POWELL JT, GREENHALGH RM. Pathogenesis of abdominal aortic aneurysm. *Brit J Surg* 1994; **81**: 935–941.

7 PILLARY G, CHANG JB, ZITO J, COHEN JR, GERSTEN K, RIZZO A, BACH AM. Computer tomography of abdominal aortic aneurysm. *Arch Surg* 1988; **123**: 727–732.

8 MANDALAM KR, JOSEPH S, RAO VRK, GUPTA AK, UNNI NM, RAO AS, KUMAR S, SUBRAMANYAN R, HALBE S, RAO EVP, NEELAKANDHAN KS, UNIKRISHNAN M. Aortoarteritis of abdominal aorta: an angiographic profile in 110 patients. *Clin Rad* 1993; **48**: 29–34.

9 CRONENWETT JL, MURPHY TF, ZELENOCK GB, WHITEHOUSE VM, LINDERNAUER SM, GRAHAM LM, QUINT LE, SILVER TM, STANLEY JC. Actuarial analysis of variables associated with rupture of small abdominal aortic aneurysms. *Surgery* 1985; **98**: 472–483.

10 O'HARA PJ, HERZER NR, KRAJEWSKI LP, TAN M, XIONG X, BEVEN EG. Ten years experience with abdominal aortic aneurysm repair in octogenarians: early results and late outcome. *J Vasc Surg* 1995; **21**: 830–926.

11 JOHNSTON KW. Multicenter prospective study of nonrupture abdominal aortic aneurysm. Part II. Variables predicting morbidity and mortality. *J Vasc Surg* 1989; **9**: 437–447.

12 BROWN PM, PATTENDEN R, VERNOOY C, ZELT DT, GUTELIUS JR. Selective management of abdominal aortic aneurysm in a prospective measurement program. *J Vasc Surgery* 1996; **23**: 213–222.

13 INZOLI F, BOSCHETTI F, ZAPPA M, LONGO T, FUMERO R. Biomechanical factors in abdominal aortic aneurysm rupture. *Eur J Vasc Surg* 1993; **7**: 668–674.

14 MACSWEENEY STR, YOUNG G, GREENHALGH RM, POWELL JT. Mechanical properties of the aneurysmal aorta. *Br J Surg* 1992; **79**: 1281–1284.

15 LANG RM, CHOLLEY BP, KORCARZ C, MARCUS RH, SHROV SG. Measurement of regional elastic properties of the human aorta. *Circulation* 1994; **90**: 1875–1882.

16 SONESSON B, LANNE T, VERNERSSON E, HANSEN F. Sex difference in the mechanical properties of the abdominal aorta in human beings. *J Vasc Surg* 1994; **20**: 959–969.

17 SALZAR RS, THUBRIKAR MJ, EPPINK RT. Pressure-induced mechanical stress in the carotid artery bifurcation: a possible correlation to atherosclerosis. *J Biomech* 1995; **28**: 1332–1341.

18 HE CM, ROACH MR. The composition and mechanical properties of abdominal aortic aneurysms. *J Vasc Surg* 1994; **20**: 6–13.

19 RAMM E. Strategies for tracing the non-linear response near limit points. In: Wunderlich E, Stein E, Bathe KJ, eds. *Non-linear Finite Element Analysis in Structural Mechanics*. Berlin: Springer-Verlag, 1981.

20 POWELL G, SIMONS J. Improved iterative strategy for non-linear structures. *Int J of numerical methods in engineering* 1981; **17**: 1455–1467.

21 MOHAN D, MELVIN JW. Failure properties of passive human aortic tissue. I-Uniaxial tension tests. *J Biomechanics* 1982; **15**: 887–902.

22 CASTRUCCI M, MELLONE R, VANZULLI A, DE GASPARI A, CASTELLANO R, ASTORE D, CHIESA R, GROSSI A, DEL MASHIO A. Mural thrombi in abdominal aortic aneurysm: MR imaging characterisation useful before endovascular treatment? *Radiology* 1995; **197**: 135–139.